

*Full Paper*

## **Solid Contact Potentiometric Sensor for The Assay of Loperamide Hydrochloride in Its Pharmaceutical Formulation and Spiked Plasma Samples**

**Maha Mahmoud Ibrahim,<sup>1,\*</sup> Khadiga Mohamed Kelani,<sup>1,2</sup> Nesreen Khamis Ramadan,<sup>2</sup> Eman Saad Elzanfaly,<sup>2,3</sup> and Ahmed Sayed Saad,<sup>2,4,\*</sup>**

<sup>1</sup>*Analytical Chemistry Department, Faculty of Pharmacy, Modern University for Technology and Information, Cairo, Egypt*

<sup>2</sup>*Analytical Chemistry Department, Faculty of Pharmacy, Cairo University, PO box 11562, Cairo, Egypt*

<sup>3</sup>*Pharmaceutical Chemistry Department, Faculty of Pharmacy and Drug Technology-Egyptian Chinese University, Cairo, Egypt*

<sup>4</sup>*Medicinal Chemistry Department, PharmD Program, Egypt-Japan University of Science and Technology (E-JUST), New Borg El-Arab City, Alexandria, 21934, Egypt*

\*Corresponding Author, Tel.: +20 100 400 9443

E-Mails: [Maha\\_Habiba2012@hotmail.com](mailto:Maha_Habiba2012@hotmail.com); [ahmed.bayoumy@pharma.cu.edu.eg](mailto:ahmed.bayoumy@pharma.cu.edu.eg); [ahmed.s.saad@ejust.edu.eg](mailto:ahmed.s.saad@ejust.edu.eg)

*Received: 20 July 2022 / Received in revised form: 1 October 2022 /*

*Accepted: 5 October 2022 / Published online: 31 October 2022*

---

**Abstract-** Computational chemistry induced several fast, cost-effective revolutionary solutions for chemistry laboratories. The reliability of such solutions has been questioned in several studies. The current work introduces an experimental validation for the computational selection of an ionophore during potentiometric sensor optimization. We studied the correlation of the experimental sensor performance parameters to the computational binding scores of the embedded ionophores and the drug (loperamide hydrochloride). The study included eight sensors of different PVC-membrane compositions. The PVC-membrane containing phosphotungstic acid, dioctyl phthalate, and carboxymethyl- $\beta$ -cyclodextrin developed a Nernstian slope of 59.69 mV/decade and a detection limit of  $2.95 \times 10^{-7}$  mol L<sup>-1</sup>. The sensor demonstrated a fast and stable response within a linear range of  $2.99 \times 10^{-6}$ - $9.09 \times 10^{-3}$  mol L<sup>-1</sup>. We examined the drug-ionophore binding using molecular modeling and docking. The docking scores (binding energy) of the cyclodextrin derivatives strongly correlate to the studied sensors'

experimental performance parameters (Nernstian slope). Performance and validation parameters were computed, and the results were statistically comparable to those of the reported method. Practically, the absence of sample preparation, chromatographic separation, high-purity solvents, and costly instrumentation are incomparable advantages of the developed method relative to the reported ones.

**Keywords-** Loperamide HCl; Glassy carbon electrode; ISE-potentiometry; Optimization; Sensor; Computational ionophore selection

## 1. INTRODUCTION

Due to their leading merits, ion-selective electrode (ISE) potentiometric sensors have been invading various fields [1–3]. Portability, real-time, and direct analysis offered by ISE-potentiometry substantiate evidence-driven decisions and on-site corrective actions. These features promise to find novel applications within industrial, environmental, and clinical fields. Literature shows several publications expressing the employment of modern potentiometric bench-top analyzers for real-time monitoring of active principle ingredients [4–13]. Literature reveals several analytical techniques for the assay of an official drug [14,15] loperamide hydrochloride (LOP) (Figure 1) [16–28]. Most reported methods employ non-aqueous solvents, hazardous chemicals, and derivatization procedures, require sophisticated instrumentation, sampling step, sample transfer, and sample preparation, and do not fit for real-time analysis. In contrast to solid-state sensors, liquid membrane sensors are more prone to mechanical damage and require care during use and storage. Additionally, the inner filling solution requires optimization for each application to reduce the membrane's passive zero-current ion flow into the aqueous solution. The solid-state sensor's ability to minimize the ion flux guarantee better operation performance and improves detection limits compared with liquid inner contact sensors.

Literature reports using several solid substrates in potentiometric sensor fabrication, such as platinum, aluminum, copper, and graphite. In addition, we employed a glassy carbon electrode (GCE) contact. The broad potential window, abundant surface chemistry, negligible background current, and suitability for a wide range of analytical applications make it an excellent solid contact for ISE-potentiometric sensors.

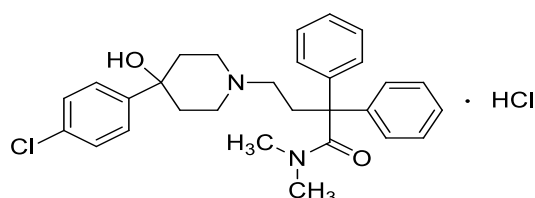


**Figure 1.** Chemical structure of loperamide hydrochloride

The current work intends to correlate the computational scores to the experimental sensor performance parameters during ionophore selection. We studied eight membrane cocktails of

varying compositions to reach the optimum membrane recipe. The recipes reside on a solid contact of glassy carbon. The solid-state potentiometric sensor was used for portable, real-time analysis of LOP in pharmaceutical and clinical applications. The rigid solid-state sensor was validated for the quantitative assay of the analyte in different sampling matrices.

## 2. EXPERIMENTAL

### 2.1. Apparatus

The potential and pH measurements were performed using Jenway potentiometer/pH meter (3510, UK), Orion Ag/AgCl double junction reference electrode (900200, USA), Jenway pH glass electrode (924001, UK), Metrohm glassy carbon electrode (6.1204.300, Switzerland), and WiseStir® magnetic stirrer (MSH-20D, Korea).

### 2.2. Chemicals and reagents

#### 2.2.1. Standards and samples

Standard LOP was obtained from the National Organization for Drug Control and Research (NODCAR) with a certified purity of 99.24%. All chemicals and solvents used were of analytical grade. Bi-distilled water was used as a solvent. Potassium tetrakis (4-chlorophenyl) borate (KTCBP), ammonium reineckate (RK), sodium tetraphenylborate (TPB), sodium phosphotungstate tribasic hydrate (PT), dioctyl phthalate (DOP), nitrophenyl octyl ether (NPOE),  $\beta$ -cyclodextrin ( $\beta$ -CD), hydroxypropyl  $\beta$ -cyclodextrin (HP $\beta$ -CD), carboxymethyl  $\beta$ -cyclodextrin (CM $\beta$ -CD), polyvinyl chloride (high molecular weight) (PVC) and tetrahydrofuran (THF) were obtained from Sigma-Aldrich. El-Nasr pharmaceutical chemical company, Cairo, Egypt, supplied the sodium hydroxide and hydrochloric acid. The pH of a 5 mmol L<sup>-1</sup> KH<sub>2</sub>PO<sub>4</sub> solution was adjusted to 4.50 to prepare the phosphate buffer. Vacsera supplied the plasma used in biological applications. All solutions were prepared in bi-distilled water.

#### 2.2.2. Pharmaceutical formulation

Imodium® tablet (batch number 8IV133) was purchased from the local market and contained 2.00 mg of LOP per tablet as claimed by the manufacturer (Catalent UK Swindon Zydis Ltd Frankland Road, Blagrove Swindon, Wiltshire).

### 2.3. Procedure

#### 2.3.1. Solutions

A stock standard solution of LOP ( $1.00 \times 10^{-2}$  mol L<sup>-1</sup>) was prepared using bi-distilled water as a solvent. Serial dilutions were carried out for the latter using phosphate buffer pH 4.50 to prepare the LOP working standard solutions ( $1.00 \times 10^{-6}$ - $1.00 \times 10^{-3}$  mol L<sup>-1</sup>).

### 2.3.2. Sensor fabrication

Eight PVC membrane cocktails (5-mL) were prepared by transferring accurately weighed amounts of the membrane components, including 213.70 mg PVC, 450.00 mg plasticizers (DOP and NPOE), 11.30 ion-exchangers (KTCBP, RK, TPB, and PT), and 11.30 mg ionophores ( $\beta$ -CD, HP $\beta$ -CD, and CM $\beta$ -CD) into eight, 5-mL volumetric flask. The components were utterly dissolved in THF; the same solvent was used to complete the volume. In addition, a 100  $\mu$ L membrane cocktail volume for each solution was cast over a polished GCE surface to prepare eight electrodes with different compositions, as shown in (Table 1).

**Table 1.** Membrane composition of the studied sensors for the determination of LOP

Membrane No.	PVC%	Plasticizer		Ion exchanger		Ionophore	
		Type	%w/w	Type	%w/w	Type	%w/w
1	31.66	DOP	66.67	KTCBP	1.67	-	-
2	31.66	DOP	66.67	RK	1.67	-	-
3	31.66	DOP	66.67	TPB	1.67	-	-
4	31.66	DOP	66.67	PT	1.67	-	-
5	31.66	NPOE	66.67	PT	1.67	-	-
6	31.15	DOP	65.67	PT	1.64	$\beta$ -CD	1.64
7	31.15	DOP	65.67	PT	1.64	HP $\beta$ -CD	1.64
8	31.15	DOP	65.67	PT	1.64	CM $\beta$ -CD	1.64

### 2.3.3. Sensor optimization

The optimization endorsed the study of eight sensors with different membrane compositions. The study evaluated the impact on the sensor performance using different ion exchangers (KTCBP, RK, TPB, and PT) and plasticizers (DOP and NPOE). The ionophore (IP) effect was assessed using three host-guest ionophores ( $\beta$ -CD, HP $\beta$ -CD, and CM $\beta$ -CD).

### 2.3.4. Molecular docking studies

The docking study justifies and substantiates the experimental work and explains the studied sensors' inferior and superior performance. The Molecular Operating Environment 2014.10 (Chemical Computing Group, Montreal, QC, Canada) investigated the interaction of LOP with  $\beta$ -CD, CM $\beta$ -CD, and HP $\beta$ -CD. The 3D structure of  $\beta$ -CD was taken from the protein complex of alpha-amylase (PDB code: 1jl8) [29], which was taken from the Brookhaven PDB and used as a template for other CDs. We used the MOE Builder function to substitute the primary -OH groups to build CM $\beta$ -CD and HP $\beta$ -CD structures [30]; we added hydrogens and minimized the structure using the MOE Quick Prep protocol; then, we reduced the potential energy of the structure using the appropriate force field AMBER 10 [31]; finally, we applied the default docking protocol [32]. The Triangle Matcher method was used to fit the ligand into

the position, and the London G scoring function was used to put the ligands in order. The docking scores were used to rank the resulting poses to select the best position.

### 2.3.5. Sensor calibration

For each prepared sensor, the potential measurements -in millivolts- were performed within the LOP standard solutions against the reference electrode at a 500-rpm stirring rate. The calibration graphs were made to express the relationship between the measured potentials (mV) and each sensor's logarithm of the molar concentration.

### 2.3.6. Effect of pH

We tracked the change in the potential developed by sensor 8 in LOP standard solutions ( $1.00 \times 10^{-6}$  -  $1.00 \times 10^{-5}$  mol L<sup>-1</sup>) while changing the pH. The pH changes were induced using NaOH and HCl ( $1.00 \times 10^{-1}$  mol L<sup>-1</sup>) solutions.

### 2.3.7. Sensor selectivity

The separate-solution method suggested by IUPAC was used to figure out the potentiometric selectivity coefficient ( $K_{LOP,int}^{pot}$ ) for common cationic contaminants [33,34].

### 2.3.8. Response time

We recorded the change in the potential with a solution after successive additions of LOP stock solution ( $1.00 \times 10^{-3}$  mol L<sup>-1</sup>). The time required for the sensor to reach the equilibrium potential ( $\pm 1$  mV) was recorded after each addition.

### 2.3.9. Application

#### 2.3.9.1. Imodium® Tablets

We obtained the average weight of ten Imodium® tablets; then, the tablets were finely powdered. An accurately weighed amount of the latter, equivalent to 5.135 mg LOP, was transferred into a 100-mL volumetric flask. Then the volume was completed by phosphate buffer pH 4.50, stirred at 500 rpm for 10 minutes to obtain a final concentration of ( $1.00 \times 10^{-4}$  mol L<sup>-1</sup>). The potential readings in mV are used to calculate the concentration from the corresponding regression equation.

#### 2.3.9.2. Spiked plasma samples

Calibration curves were recorded in plasma, and the response parameters were calculated (slope, linear range, and LOD). One milliliter of plasma was put into a 25-milliliter beaker, spiked with a known amount of LOP standard. The spiked plasma samples were diluted using phosphate buffer pH 4.50. The potential was recorded in mV using sensor 8. The standard addition method was used to determine the sample solution's concentration. We recorded the change in potential after adding one milliliter of a  $1.00 \times 10^{-3}$  mol L<sup>-1</sup> LOP solution, and the following equation was used to calculate the sample concentration:

$$C_u = \frac{C_s V_s}{(V_T \times 10^{\Delta E/s}) - V_u}$$

where  $C_u$  and  $C_s$  are the concentration of the unknown and the standard solution,  $V_u$ ,  $V_s$ , and  $V_T$  are the unknown, standard, and total solution volume.  $\Delta E$  is the change in the potential, while  $(s)$  is the slope of the employed sensor. Within a 95% confidence interval, statistical F-ratio and Student's t-tests compared the developed method to the reported chromatographic method [24].

### 3. RESULTS AND DISCUSSION

Their rewarding sensitivity and selectivity of potentiometric sensors fit a wide range of analytical applications. For example, ISE-potentiometry is one of the few non-destructive techniques that comply with outdoor investigations' direct analysis and portability requirements [35].

#### 3.1. Sensor optimization

The PVC-membrane cocktail recipe and the working conditions affect sensor performance. The ion exchanger controls analyte-extraction kinetics at the membrane-sample interface and offers a primitive selectivity compared to the ionophore. The selective ionophore-analyte interaction strongly contributes to sensor selectivity. The plasticizer is the most abundant membrane component. By controlling membrane polarity, a plasticizer acts as the doorman to regulate transport in and out across the membrane gateways. In consequence, the type and amount of plasticizer affect membrane selectivity and lifetime. Experimental conditions, e.g., sample pH, should be controlled to guarantee the exchange of the ionized analyte at the membrane-sample interface. The optimization process evaluates the Effect of each factor on the response to drive the selection of membrane constituents, cocktail proportions, and experimental conditions that guarantee optimal sensor performance [36,37].

#### 3.2. Molecular docking studies

Computational chemistry (molecular modeling and molecular docking) evaluated the interaction of LPR within the cyclodextrins' cavity [38]. A longer hydrophobic chain connected to -CD improves drug assembly in complex [39]. Furthermore, guest hydrophobicity affects CD complexation [40,41]. LOP forms inclusion complexes with the studied cyclodextrins. The LOP binding energies with  $\beta$ -CD, CM $\beta$ -CD, and HP $\beta$ -CD were found to be -7.28, -8.13, and -7.39 Kcal/mol, respectively.

Interestingly, experimental results proved superior performance for the CM $\beta$ -CD. The binding of CM $\beta$ -CD is stronger and more favorable than the other  $\beta$ -CD derivatives due to its hydrophobicity, as shown and explained in Figure 2 (A, B, and C). Experimentally, CM $\beta$ -CD

produced the best Nernstian slope, shortest response time, and lowest detection limits relative to the other CD derivatives. The experimental results complied with the computational calculations.

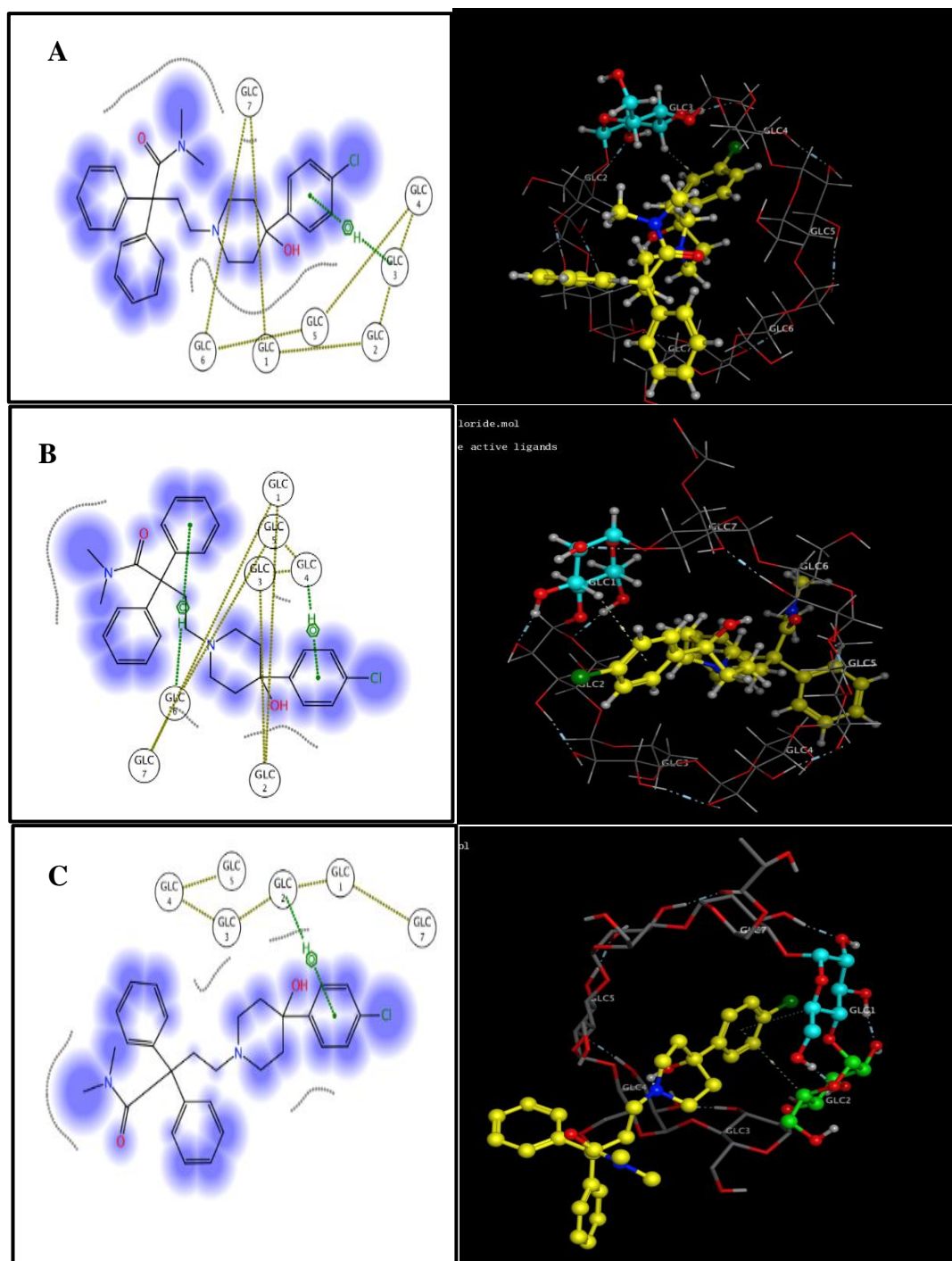


**Figure 2.** 2D and 3D Binding mode of LOP (yellow ball and sticks) into  $\beta$ -CD (A), CM $\beta$ -CD (B), and HP $\beta$ -CD (C)

Ion exchangers are lipophilic compounds with ionic sites that can freely exchange and equilibrate their counterions (Analyte) at the membrane-solution interface according to the analyte ion activity in the sample solution  $a_{aq}$  and the membrane  $a_m$ . This is balanced by a phase boundary potential ( $E$ ) that builds up at the membrane-solution interface as the charges are separated. Assuming constant analyte activity in the membrane, a Nernstian response is developed as follows:

$$E = K + \frac{RT}{nF} \ln a_{aq}$$

where  $K$  is a constant,  $R$  is the gas constant,  $F$  is the Faraday constant,  $T$  is the absolute temperature, and  $n$  is the ionic charge.

Ion exchangers dope ionic sites into the membrane matrix. This lets analytes move between the membrane and the sample and lowers the resistance of the membrane. Owing to its basic nature, LOP possesses a predominant cationic nature in neutral and acidic media ( $pK_a$  9.41) [42]. We examined the performance of four different ion exchangers. PT proved the best Nernstian slope and lowest detection limit. The low detection limit demonstrates better selectivity, as the LOD is theoretically reached when half of the analyte ions are displaced from the membrane matrix [43,44], as shown in Table 2.

Plasticizers solubilize membrane constituents and modify the membrane polarity, control the exchange at the membrane sample interface and determine the sensor lifetime. We studied two different plasticizers (DOP (sensor 4) and 2-NPOE (sensor 5)), as shown in Table 1. Plasticizing using DOP enhanced membrane permeability and thus improved membrane performance, as indicated by the near-Nernstian slope (64.48 mV/decade), shorter response time, and better response stability, as shown in Table 2. Plasticizers modify the polarity of the PVC membrane to facilitate the exchange of the analyte ion at the sensor sample interface. The relatively low dielectric constant of DOP modified the membrane polarity to reduce Gibb's free energy of LOP ion transfer and enabled faster and more stable exchange kinetics.

Ionophores are selective complexing agents doped within the membrane matrix to host the analyte and enhance the sensor selectivity. Lipophilic ionophores selectively incorporate the analyte into the membrane and suppress competition with interfering ions. Thus, preserving the activity of the membrane phase ( $a_m$ ) as the activity in the sample ( $a_{aq}$ ) is changed [37]. Accordingly, the developed potential ( $E$ ) will depend only on the ionic activity in the aqueous sample solution according to the following equation [37]:

$$E = \frac{RT}{nF} \ln \frac{k_m a_{aq}}{a_m}$$

where  $R$  is the gas constant,  $F$  is the Faraday constant,  $T$  is the absolute temperature,  $n$  is the ionic charge and  $k_m$  is a constant that considers Gibb's free energy of the transfer of analyte ions from the aqueous phase to the organic phase.



Recent ion-selective electrodes have been introduced with exceptionally higher selectivity and lower detection limits thanks to the ionophores. The latter are incorporated in polymeric membranes as selective complexing agents that contain only the analyte ion in the membrane and suppress competition from interfering ions [43]. Carboxymethyl—cyclodextrin (CM-CD) is employed in enantiomer recognition and separation technologies. CM-CD is used to generate nanocarriers and transfect nucleic acids. Based on the obtained results, we selected CM $\beta$ -CD (sensor 8) as the ionophore of choice for the LOP-selective membrane (Table 2). Sensor 8 containing CM $\beta$ -CD demonstrated the best Nernstian slope, lowest detection limit, and fastest slope. This indicates the ability of CM $\beta$ -CD to form a more stable complex with LOP than either  $\beta$ -CD or HP $\beta$ -CD and thus hold the concentration of LOP constant within the membrane and prevent LOP ion infiltration into the aqueous sample solution (Figure 3).

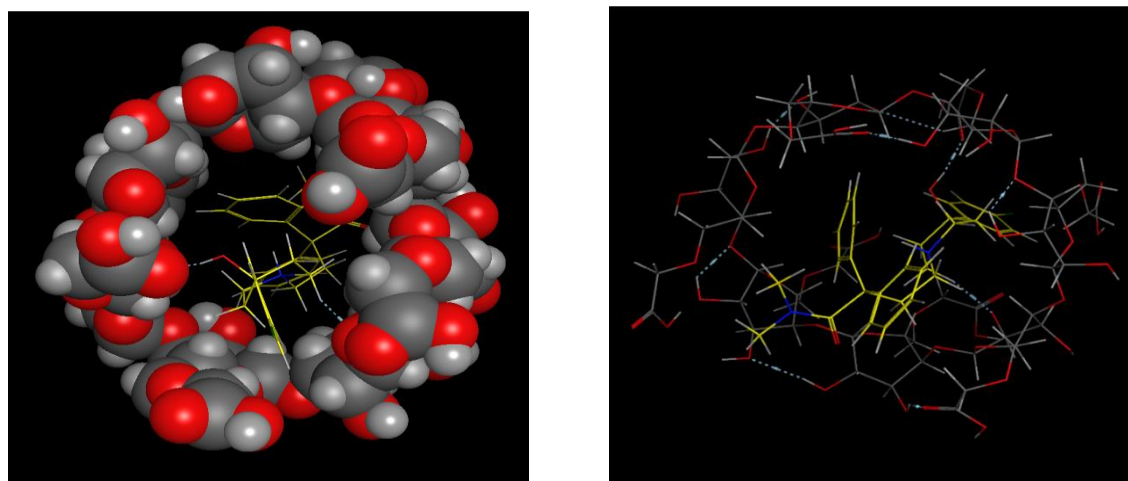


**Figure 3.** The 3D chemical structure of the host-guest inclusion complex formed between LOP (Yellow structure) and CM $\beta$ -CD, showing an energetically favored orientation of LOP within the cavity of CM $\beta$ -CD

Calibration curves relating the logarithmic function of the molar concentration relative to the measured potential were recorded for the eight sensors over six weeks, as shown in Figure 4 and Table 2.

Sensor performance parameters were calculated using IUPAC recommendations. (slope, LOD, response time, and lifetime) [33,34]. Sensor 8 proved the best Nernstian slope (59.69 mV/decade), lowest detection limit ( $2.95 \times 10^{-7}$  mol L $^{-1}$ ), and fastest response time (15 s) among the tested sensors. Sensor validation followed ICH criteria [45] (Table 2). Accordingly, sensor eight was selected to complete the study.

The sensor has a better Nernstian slope, greater linear range, and lower detection limit than those mentioned in the literature [24].

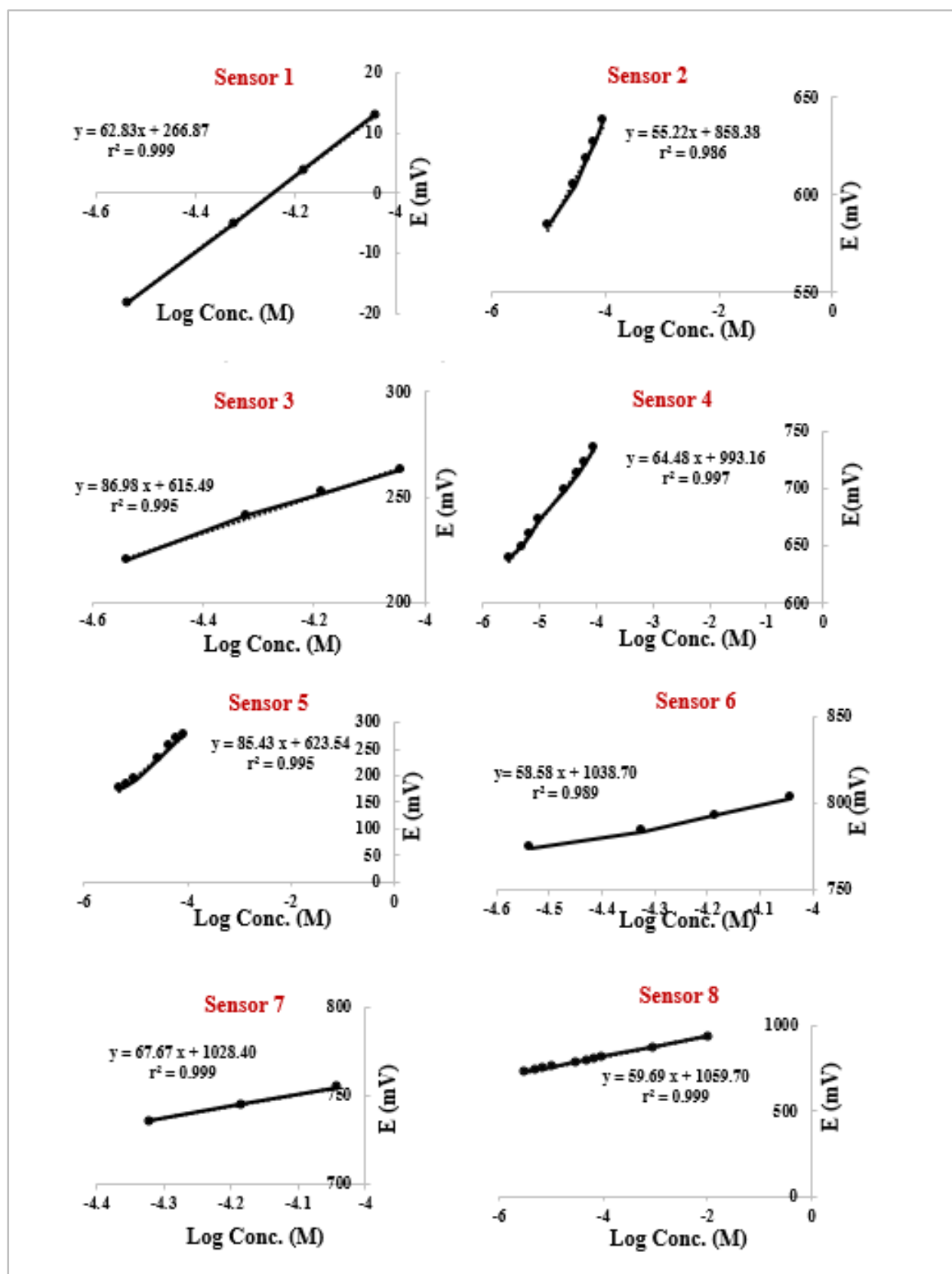


Figure 4. Potential profile of the studied sensors

**Table 2.** The investigated sensors' performance characteristics were as follows

Parameter <sup>a</sup>	Sensor 1	Sensor 2	Sensor 3	Sensor 4	Sensor 5	Sensor 6	Sensor 7	Sensor 8
<b>Slope</b> (mV/decade)	62.83	55.22	86.98	64.48	85.43	58.58	67.67	59.69
<b>Intercept</b> (mV)	266.87	858.38	615.49	993.16	623.54	1038.70	1028.40	1059.70
<b>Correlation coefficient (r)</b>	0.999	0.986	0.995	0.997	0.995	0.989	0.999	0.999
<b>Concentration range (M)</b>	2.91×10 <sup>-5</sup> - 9.09×10 <sup>-5</sup>	9.90×10 <sup>-6</sup> - 9.09×10 <sup>-5</sup>	2.91×10 <sup>-5</sup> - 9.09×10 <sup>-5</sup>	2.99×10 <sup>-6</sup> - 9.09×10 <sup>-5</sup>	4.98×10 <sup>-6</sup> - 9.09×10 <sup>-5</sup>	2.91×10 <sup>-5</sup> - 9.09×10 <sup>-5</sup>	2.91×10 <sup>-5</sup> - 9.09×10 <sup>-5</sup>	2.99×10 <sup>-6</sup> - 9.09×10 <sup>-3</sup>
<b>Working pH range</b>	2.00– 6.50							
<b>Response Time (s)</b>	20-120	20-180	15-120	10-20	10-60	10-50	10- 50	5-15
<b>LOD (M)</b>	9.38×10 <sup>-6</sup>	5.99×10 <sup>-6</sup>	2.99×10 <sup>-6</sup>	1.95×10 <sup>-6</sup>	4.98×10 <sup>-6</sup>	4.17×10 <sup>-6</sup>	1.19×10 <sup>-7</sup>	2.95×10 <sup>-7</sup>
<b>Average accuracy ± SD</b>	100.01±0.06	100.01±0.99	100.00±0.31	99.94±0.59	110.40±2.92	100.00±0.49	100.12±0.24	99.99±0.30
<b>Repeatability (±%RSD)</b>	±0.362	± 0.393	±0.402	±1.030	±2.650	±0.490	±0.241	±0.301
<b>Intermediate Precision (±%RSD)</b>	±0.360	± 0.952	±0.411	±1.391	±2.643	±0.482	±0.202	±0.320
<b>Stability (weeks)</b>	4	4	4	6	4	5	5	6

<sup>a</sup> Average of three determinations

### 3.3. Effect of pH

Owing to the weak basic nature of LOP (basic  $pK_a=9.41$ ) [42], it was mandatory to check the operating pH range at which LOP is predominantly present in its cationic form to achieve optimal analytical conditions. Figure 5 shows the potential-pH profile for  $1.00 \times 10^{-6}$ – $1.00 \times 10^{-5}$  mol L<sup>-1</sup> LOP (Sensor 8). The sensor developed a constant potential within the pH range of 2.00–6.50. At pH lower than 2.00, drift in the potential reading results from the competition of protons on the cationic sites. At pH values higher than 6.50, the unionized free loperamide base separates from the solution, and the concentration of LOP declines gradually.

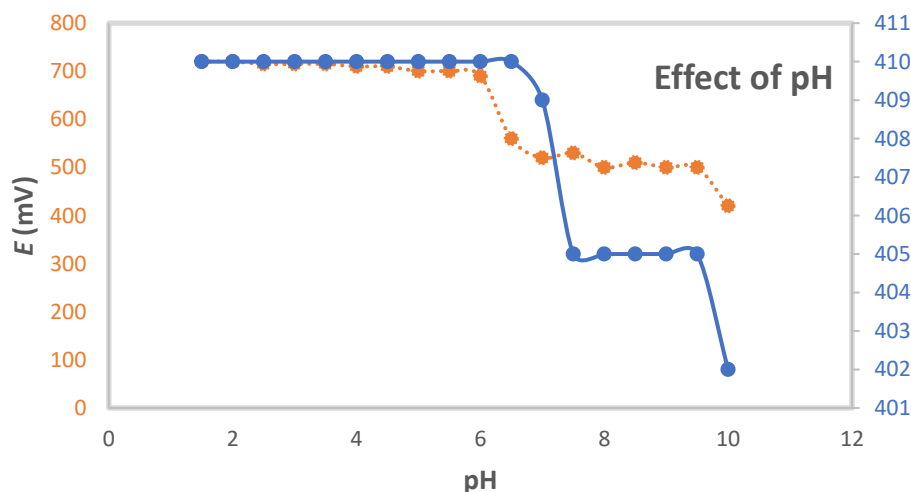


**Figure 5.** Effect of pH on the response of the sensor 8 in LOP  $1.00 \times 10^{-5} \text{ ml L}^{-1}$ (....) and  $1.00 \times 10^{-6} \text{ mol L}^{-1}$ (—) M solutions [working pH range: 2.00-6.50]

### 3.4. Sensor selectivity

We examined the response of sensor 8 to the tablet excipients, organic substances, and other related substances. Results showed that the proposed sensor was highly selective, without substantial interference from interfering species, as shown in Table 3.

**Table 3.** Potentiometric selectivity coefficients ( $K_{LOP,interferent}^{pot}$ ) of the selected sensor using the separate solutions method (SSM)

Interferent <sup>a</sup>	Selectivity Coefficients <sup>b</sup>
MnCl <sub>2</sub>	$9.37 \times 10^{-3}$
CaCl <sub>2</sub>	$7.43 \times 10^{-3}$
CoSO <sub>4</sub>	$5.04 \times 10^{-4}$
ZnSO <sub>4</sub>	$5.66 \times 10^{-3}$
Pb (CH <sub>3</sub> COO) <sub>2</sub>	$7.43 \times 10^{-3}$
MgSO <sub>4</sub>	$1.31 \times 10^{-4}$
KCl	$3.42 \times 10^{-3}$
BaCl <sub>2</sub>	$1.31 \times 10^{-3}$
NaCl	$8.89 \times 10^{-3}$
CuSO <sub>4</sub>	$6.04 \times 10^{-3}$
FeSO <sub>4</sub>	$1.31 \times 10^{-4}$
NH <sub>4</sub> Cl	$1.56 \times 10^{-3}$
NiSO <sub>4</sub>	$7.05 \times 10^{-3}$

<sup>a</sup> Measured in  $10^{-3} \text{ M}$  solutions

<sup>b</sup> Average of three determinations

### 3.5. Response time

The response was scanned for different successive concentrations as a function of time. Results demonstrated a stable and fast response of the developed sensor for different concentrations of LOP. However, results also show that the membrane is more responsive to higher concentrations than lower ones, as shown in Figure 6.

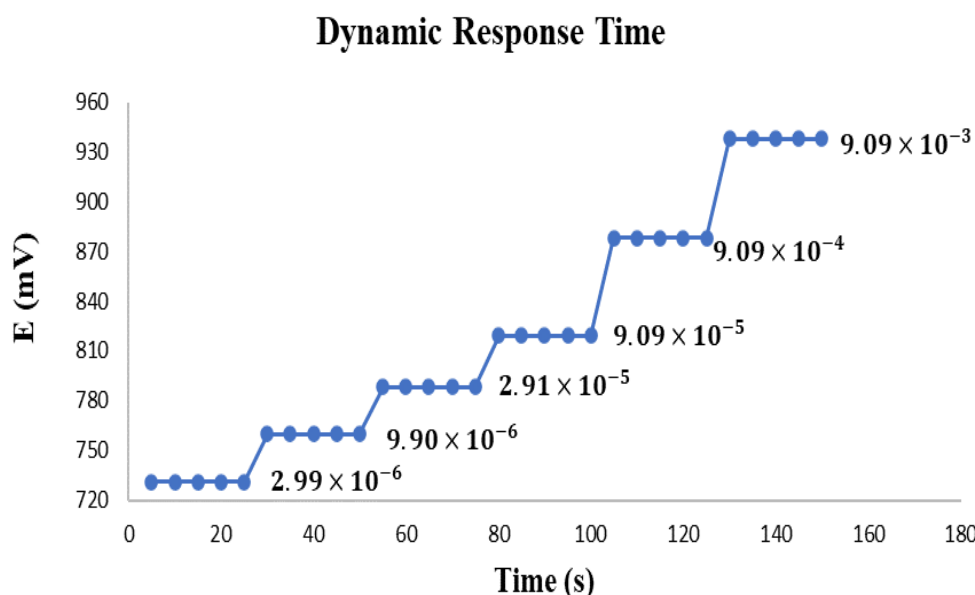


**Figure 6.** Dynamic response time of sensor 8 towards different concentrations of LOP

### 3.6. Analytical application in pharmaceutical formulation

The newly suggested sensor with higher performance and features (sensor 8) was used to measure LOP in pharmaceutical formulation preparations (Imodium® Tablets) and spiked human plasma samples to demonstrate the applicability of electrodes for potential analytical applications. The sensor recovered LOP accurately and precisely, whereas tablet excipients did not interfere, as shown in Table 4. The results illustrate the usability of the developed sensor for LOP assay without prior treatment, separation, or extraction. By comparing the obtained results using the developed ISE potentiometric method to the reported method [24], it was found that no significant difference was noticed between both methods, as shown in Table 5.

**Table 4.** Determination of loperamide HCl in pharmaceutical dosage form and spiked plasma sample using Sensor 8

Pharmaceutical Formulation	Recovery% <sup>a</sup> ± SD
Imodium® tablets" Batch no." (310098B)	99.24 ± 1.180
Spiked plasma samples	98.50 ± 1.901

<sup>a</sup> Average of five determinations

**Table 5.** Statistical comparison of the proposed potentiometric method and the reported HPLC method [27] for determining LOP in pure powder form

Parameters	Sensor 8	*Reported method [27]
Mean	99.99	99.76
RSD%	0.301	0.420
n	9	9
Variance	0.09	0.17
**F-value	1.96	<b>f-tabulated</b> 3.18
**Student's t-test	0.79	<b>Tabulated t-value</b> 2.26

\*HPLC method using Inertsil-ODS 3V, C18, 100 × 4.6 mm, 5μ column. Acetonitrile: buffer: 1.00 M NaOH (390: 610: 0.5, v/v/v) as mobile phase, UV detection at 224.0 nm and a flow rate 1.50 ml/min.

\*\*Significance level (P=0.05)

#### 4. CONCLUSION

The computational scores for the binding energy of the three different cyclodextrin ionophores and the analyte effectively correlate to the experimental Nernstian slope of the sensors containing these ionophores. Computational ionophore-analyte binding energies may serve as a potential estimate for ionophore selection. Additional studies are required on different ionophore classes and other sensor components to substantiate our conclusion. Computational selection saves time, chemicals, lab resources, and efforts exerted in additional optimization experiments. The proposed method successfully determined LOP in its pure powder form, pharmaceutical dosage formulation, and spiked human plasma samples without prior treatment, separation, or extraction. The sensor represents a promising alternative eco-friendly tool for LOP determination and quality control laboratories.

#### Conflict of interest

This research received no specific grant from public, commercial, or not-for-profit funding agencies.

#### Acknowledgment

The authors would like to thank Dr. Asmaa M. Aboulmagd & Dr. Rehab Hamed for their significant contribution to the docking.

**REFERENCES**

- [1] A.S. Fayed, R.M. Youssif, H.A.M. Hendawy, N.N. Salama, and E.S. Elzanfaly, *J. Electrochem. Soc.* 165 (2018) B730.
- [2] R. Rosenberg, M.S. Bono, S. Braganza, C. Vaishnav, R. Karnik, and A.J. Hart, *Plos one* 13 (2018).
- [3] J. Juárez-Gómez, M.T. Ramírez-Silva, M. Romero-Romo, E. Rodríguez-Sevilla, F. Pérez-García, and M. Palomar-Pardavé, *J. Electrochem. Soc.* 163 (2016) B90.
- [4] E.S. Elzanfaly, and A.S. Saad, *ACS Sustainable Chemistry and Engineering* 5 (2017).
- [5] M.K.A. El-Rahman, M.R. Rezk, A.M. Mahmoud, and M.R. Elghobashy, *Sens. Actuators B* 208 (2015) 14.
- [6] M.A. Basha, M.K. Abd El-Rahman, L.I. Bebawy, and M.Y. Salem, *Chinese Chem. Lett.* 28 (2017) 612.
- [7] E.S. Elzanfaly, S.A. Hassan, M.Y. Salem, and B.A. El-Zeany, *Sens. Actuators B* 228 (2016) 587.
- [8] M.K.A. El-Rahman, H.E. Zaazaa, N.B. Eldin, and A.A. Moustafa, *Talanta* 132 (2015) 52.
- [9] S. Makarychev-Mikhailov, A. Shvarev, and E. Bakker, *Electrochem. Sens.* (2008) 71.
- [10] G. Li, X. Lyu, Z. Wang, Y. Rong, R. Hu, Z. Luo, and Y. Wang, *Measurement Sci. Technol.* 28 (2017) 025104.
- [11] A.S. Saad, I.A. Naguib, M.E. Draz, H.E. Zaazaa, and A.S. Lashien, *J. Electrochem. Soc.* 165 (2018) H764.
- [12] S.A. Boltia, A.T. Soudi, E.S. Elzanfaly, and H.E. Zaazaa, *J. Electrochem. Soc.* 166 (2019) B141.
- [13] M.R. Rezk, A.S. Fayed, H.M. Marzouk, and S.S. Abbas, *J. Electrochem. Soc.* 164 (2017) H628.
- [14] B. O'Malley, *European Pharmacopoeia, British Medical Journal.* 4 (1971) 815.
- [15] J.C. Hung, USP general chapter <797> pharmaceutical compounding-sterile preparations., *Journal of Nuclear Medicine : Official Publication, Society of Nuclear Medicine*, 45 (2004).
- [16] H.J. Leis, and H. Gleispach, *Journal of Chromatography B: Biomedical Sciences and Applications*, 494 (1989) 324.
- [17] Z.A. El Sherif, A.O. Mohamed, M.I. Walash, and F.M. Tarras, *J. Pharm. Biomed. Anal.* 22 (2000) 13.
- [18] J.H. Yu, H.J. Kim, S. Lee, S.J. Hwang, W. Kim, and C.J. Moon, *J. Pharm. Biomed. Anal.* 36 (2004) 421.
- [19] S.S. Johansen, and J.L. Jensen, *J. Chromat. B* 811 (2004) 31.
- [20] B. Ganßmann, A. Klingmann, J. Burhenne, Y. Tayrouz, R. Aderjan, and G. Mikus, *Chromatographia* 53 (2001) 656.

- [21] H. He, A. Sadeque, J.C.L. Erve, A.J.J. Wood, and D.L. Hachey, *J. Chromat. B* 744 (2000) 323.
- [22] H. Chen, F. Gaul, D. Gou, and A. Maycock, *J. Pharm. Biomed. Anal.* 22 (2000) 555.
- [23] C. Leung, and C. Au-yeung, *J. Chromat.* 449 (1988) 341.
- [24] H. Kabir, R.K. Paul, S. Rahaman, F. Ahmad, D.K. Bhattacharjya, and S. Rahaman, *Int. J. Advanced Res. Chem. Sci.* 4 (2017) 11.
- [25] I.I. Hewala, *J. Pharm. Biomed. Anal.* 13 (1995) 761.
- [26] H.M. Elqudaby, G.G. Mohamed, and G.M.G. El Din, *J. Pharmacy Res.* 7 (2013) 686.
- [27] F. Faridbod, F. Mizani, M.R. Ganjali, and P. Norouzi, *Int. J. Electrochem. Sci.* 7 (2012) 7643.
- [28] F. Salama, N. El abasawy, A. El-Olemy, M. Hasan, and M. Kamel, *J. Advanced Pharmacy Res.* 4 (2020) 46.
- [29] T. Yokota, T. Tonozuka, Y. Shimura, K. Ichikawa, S. Kamitori, and Y. Sakano, *Bioscience, Biotechnol. Biochem.* 65 (2001) 619.
- [30] S. Shityakov, R. E. Salmas, S. Durdagi, E. Salvador, K. Pápai, M. Josefa Y. Gascón, H. P. Sánchez, I. Puskás, N. Roewer, C. Förster, and J. A. Broscheit, *Journal of Chemical Information and Modeling*, ACS Publications, 56 (2016) 1914.
- [31] R.J.W. David A. Case, T. E. Cheatham III, T. Darden, H. Gohlke, R. Luo, K. M. Merz Jr., A. Onufriev, C. Simmerling, and B. Wang, *J. Computational Chem.* 26 (2005) 1668.
- [32] M.O. Radwan, S. Sonoda, T. Ejima, A. Tanaka, R. Koga, Y. Okamoto, M. Fujita, and M. Otsuka, *Bioorganic and Medicinal Chem.* 24 (2016) 4398.
- [33] IUPAC, *Recommendations for Nomenclature of Ion-Selective Electrodes*, *Pure and Applied Chem.* 48 (1976) 127.
- [34] IUPAC Recommendations, *Analytical Chemistry Division Commission on Analytical Nomenclature*, *Pure and Applied Chem.* 72 (2000) 1851.
- [35] E. Zdrachek, and E. Bakker, *Anal. Chem.* 91 (2019) 2.
- [36] A.M. El-Kosasy, M.A. Shehata, N.Y. Hassan, A.S. Fayed, and B.A. El-Zeany, *Talanta* 66 (2005) 746.
- [37] M.R. Elghobashy, and M.R. Rezk, *Anal. Bioanal. Electrochem.* 6 (2014) 461.
- [38] P. Ahmadi, and J.B. Ghasemi, *J. Inclusion Phenomena and Macrocyclic Chem.* 79 (2014) 401.
- [39] S. De Chasteigner, H. Fessi, J.P. Devissaguet, and F. Puisieux, *Drug Development Res.* 38 (1996) 125.
- [40] G. Astray, J.C. Mejuto, J. Morales, R. Rial-Otero, and J. Simal-Gándara, *Food Res. Int.* 43 (2010) 1212.
- [41] M. Kfoury, L. Auezova, S. Fourmentin, and H. Greige-Gerges, *J. Inclusion Phenomena and Macrocyclic Chem.* 80 (2014) 51.
- [42] D.S. Wishart, C. Knox, A.C. Guo, D. Cheng, S. Shrivastava, D. Tzur, B. Gautam, and



- M. Hassanali, *Nucleic Acids Res.* 36 (2008).
- [43] H.M. Abu Shawish, A.M. Khedr, K.I. Abed-Almonem, and M. Gaber, *Talanta* 101 (2012) 211.
- [44] E. Bakker, P. Bühlmann, and E. Pretsch, *Chem. Rev.* 97 (1997) 3083.
- [45] I.C.H. Guideline, *Validation of analytical procedures: methodology Q2 (R1)*, IFPMA: Geneva (2005).